Published for SISSA by Springer

Received: *April 20, 2022*
Accepted: *May 1, 2022*
Published: *May 20, 2022*

On the implications of positive W mass shift

Reuven Balkin,[a] **Eric Madge,**[b] **Tony Menzo,**[c] **Gilad Perez,**[b] **Yotam Soreq**[a] **and Jure Zupan**[c]

[a] *Physics Department, Technion — Israel Institute of Technology, Haifa 3200003, Israel*
[b] *Department of Particle Physics and Astrophysics, Weizmann Institute of Science, Rehovot 7610001, Israel*
[c] *Department of Physics, University of Cincinnati, Cincinnati, OH 45221, U.S.A.*

E-mail: reuven.b@campus.technion.ac.il, eric.madge-pimentel@weizmann.ac.il, menzoad@mail.uc.edu, gilad.perez@weizmann.ac.il, soreqy@physics.technion.ac.il, zupanje@ucmail.uc.edu

Abstract: We investigate the phenomenological implications of the recent W mass measurement by the CDF collaboration, which exhibits tension with the standard model (SM) electroweak fit. Performing the fit to the electroweak observables within the SM effective field theory, we find that the new physics that contributes either to the determination of the electroweak vacuum expectation value, or to the oblique parameters, can improve the agreement with data. The best description is obtained from a fit where flavor universality is not required in the new physics operators, with 2 to 3 σ indications for several nonzero Wilson coefficients. We point out that top partners with order TeV masses could lead to the observed shift in the W mass.

Keywords: Electroweak Precision Physics, SMEFT, Vector-Like Fermions

ArXiv ePrint: 2204.05992

https://doi.org/10.1007/JHEP05(2022)133

JHEP05(2022)133

Contents

1 Introduction

Recently, the CDF collaboration provided a legacy measurement of the W boson mass [1]

$$m_W^{\rm CDF} = (80.4335 \pm 0.0094)\,\text{GeV}\,. \tag{1.1}$$

This most precise measurement of m_W represents a shift of $3.6\,\sigma$ compared to the 2021 PDG average of the LEP [2], ATLAS [3] and the previous Tevatron combination [4], which yields $m_W^{\rm PDG} = (80.379 \pm 0.012)\,\text{GeV}$ [5]. Similarly, a naive average of LEP, ATLAS and the LHCb [6] measurement leads to $m_W^{\rm NWA} = (80.368 \pm 0.014)\,\text{GeV}$, a difference of $3.8\,\sigma$ from eq. (1.1), showing that there is significant tension between the CDF measurement and the determinations of m_W by other experiments. Working under the assumption that the CDF measurement will be confirmed by future measurements, we explore its phenomenological implications. Intriguingly, the CDF measurement is also in $\sim 7.0\,\sigma$ tension with the Standard Model (SM) prediction from a global electroweak fit, $m_W^{\rm fit} = (80.361 \pm 0.006)\,\text{GeV}$ [5]. In this paper, we perform several fits to Z and W pole observables with varying assumptions on new physics: just the operators that modify the determination of the electroweak vacuum expectation value (VEV), new physics (NP) only in the oblique corrections, or the general fit that allows also for non-universal couplings of new physics. We then interpret the results of the fits in terms of several simple new physics explanations that could bring the W measurement by CDF in agreement with the predictions from the

JHEP05(2022)133

electroweak fit. For other recent discussions of the phenomenological implications of the CDF m_W measurements see refs. [7–29].[1]

The paper is organized as follows. In section 2 we perform a general analysis of the electroweak data, including the new CDF measurement of m_W. Section 3 contains a discussion of sample new physics models that can alleviate the tension of the SM predictions with data, while section 4 contains our conclusions. Further details about the fit are collected in section A and appendix B.

2 General analysis

In performing the global fit to electroweak observables, allowing for dimension six new physics operators, we follow the approach of refs. [31, 32] (see also [33, 34] as well as the early work in [35]). First the SM electroweak fit is performed, the results of which are then used to obtain the constraints on the Wilson coefficients of dimension six operators

$$\mathcal{L}_{\text{eff}} = \mathcal{L}_{\text{SM}} + \frac{1}{v^2}\sum_i c_i \mathcal{O}_{6,i}, \tag{2.1}$$

where v is the Higgs VEV and the sum in the second term runs over the SM effective field theory (SMEFT) operators in the Warsaw basis [36]. The global χ^2 function that is used to obtain the bounds on the SMEFT Wilson coefficients is given by,

$$\chi^2 = \sum_{i,j} (O_{i,\text{exp}} - O_{i,\text{th}})\sigma_{ij}^{-2}(O_{j,\text{exp}} - O_{j,\text{th}})\,, \tag{2.2}$$

with σ_{ij}^{-2} the experimental covariance matrix, $O_{i,\text{exp}}$ the experimental meausurement of the particular electroweak observable, while its theory prediction at next-to-next-to-leading order in the SM and expanded to linear order in new physics is

$$O_{i,\text{th}} = O_{i,\text{SM}}^{\text{NNLO}} + \vec{\delta g}\cdot O_{i,\text{NP}}^{\text{LO}}\,. \tag{2.3}$$

For the SM we use the latest theory results, with the numerical values collected in ref. [34] based on [33, 37, 38], while for NP corrections it suffices to calculate to leading order. The 19 pole parameters δg_i depend on the dimension 6 Wilson coefficients, with the dependence given in appendix A of ref. [32], while the observables used in our fit are listed in table 1. The NP corrections to the observables depend on the NP Wilson coefficients as well as on the two weak gauge couplings and the electroweak vacuum expectation values,

$$g_L = 0.6458\,, \qquad g_Y = 0.3580\,, \qquad v = 246.22\,\text{GeV}\,, \tag{2.4}$$

which are obtained by using the LO SM relations for the Fermi constant $G_F = 1/(\sqrt{2}v^2)$, the Z boson mass, $m_Z = \sqrt{g_L^2 + g_Y^2}v/2$, and the fine structure constant at m_Z, $\alpha(m_Z)^{-1} = 4\pi(g_L^2 + g_Y^2)/(g_L^2 g_Y^2)$. The SM relations get corrected by the NP contributions, which is taken into account when writing the expressions for $O_{i,\text{NP}}^{\text{LO}}$ in terms of the dimension 6

[1] The quantitative analysis of whether or not these follow the universal scaling laws uncovered in [30] we defer to future work, at which point we anticipate more data to become available.

JHEP05(2022)133

Wilson coefficients. Setting all NP contributions to zero gives for the SM $\chi^2_{\rm SM} = 99.3$ with 42 observables contributing to the χ^2.

In light of the new CDF measurement of m_W, it is interesting to focus on the NP that can directly result in a shift in the W mass relative to the prediction for the Z mass. Only five dimension 6 operators result in such a shift

$$\delta m_W \equiv \frac{m_W|_{\rm exp} - m_W|_{\rm SM}}{m_W} = \frac{1}{g_L^2 - g_Y^2}\Big(- g_L^2 g_Y^2 c_{WB} + g_L^2 c_T - g_Y^2 \delta v\Big), \tag{2.5}$$

where the normalized shift in the electroweak VEV due to NP is given by[2]

$$\delta v = \frac{1}{2}([c'_{H\ell}]_{11} + [c'_{H\ell}]_{22}) - \frac{1}{4}[c_{\ell\ell}]_{1221}. \tag{2.6}$$

The corresponding operators are given by

$$\begin{aligned} \mathcal{O}_T &= (H^\dagger \overset{\leftrightarrow}{D}_\mu H)^2, & \mathcal{O}_{\rm WB} &= g_L g_Y H^\dagger \sigma^i H W^i_{\mu\nu} B_{\mu\nu}, \\ \mathcal{O}'_{H\ell} &= (\bar\ell \sigma^i \gamma_\mu \ell)(H^\dagger i\sigma^i \overset{\leftrightarrow}{D}_\mu H), & \mathcal{O}_{\ell\ell} &= (\bar\ell \gamma_\mu \ell)(\bar\ell \gamma^\mu \ell), \end{aligned} \tag{2.7}$$

where σ^i acts on the $\mathrm{SU}(2)_L$ space and we suppressed the generational indices.

2.1 New physics in the muon decay

We first explore the possibility that the NP modifies the muon lifetime, from which the Fermi constant is extracted. The main observation here is that in the electroweak fits the SM predictions for the W mass is obtained from its relation to the Fermi constant, G_F, which is very precisely determined from muon lifetime. A change to the muon lifetime due to new physics contributions then directly translates to a shift in the prediction for m_W from the electroweak fit [39, 40].

In the SM electroweak fit the W mass is predicted from the SM relation [38]

$$m_W^2|_{\rm fit} = \frac{m_Z^2}{2}\left[1 + \left(1 - \frac{\sqrt{8}\pi\alpha(1-\Delta r)}{G_F m_Z^2}\right)^{1/2}\right], \tag{2.8}$$

where m_Z and G_F are the measured Z boson mass and Fermi constant, α is the fine structure constant, and Δr are the radiative corrections that depend on the other SM parameters, including the m_W. If the total decay width of the muon, Γ_μ, receives a correction $\Delta\Gamma_\mu^{\rm NP}$ from NP,

$$\Gamma_\mu = \Gamma_\mu^{\rm SM} + \Delta\Gamma_\mu^{\rm NP}, \tag{2.9}$$

this shifts the value of G_F away from the SM, and translates to a modification of the predicted m_W

$$\delta m_W = -\frac{1}{4}\frac{m_Z^2 - m_W^2}{2m_W^2 - m_Z^2}\frac{\Delta\Gamma_\mu^{\rm NP}}{\Gamma_\mu^{\rm SM}}. \tag{2.10}$$

[2]We note the typographical error in [32] in the sign multiplying $[c_{\ell\ell}]_{1221}$.

JHEP05(2022)133

This is a special case of the more general expression, eq. (2.5), assuming here only a NP change to δv,

$$\frac{\Delta\Gamma_\mu^{\rm NP}}{\Gamma_\mu^{\rm SM}} = 4\delta v = 2([c'_{H\ell}]_{11} + [c'_{H\ell}]_{22}) - [c_{\ell\ell}]_{1221}. \tag{2.11}$$

Note that explaining the CDF m_W measurement requires a negative interference with the SM in the muon decay width,

$$\frac{\Delta\Gamma_\mu^{\rm NP}}{\Gamma_\mu^{\rm SM}} = (-9.0 \pm 1.3) \times 10^{-13}\,. \tag{2.12}$$

While in principle Γ_μ can be modified by new muon decay channels, potentially with light new physics in the final state, such contributions would always result in an increased Γ_μ. A possible explanation of the CDF m_W measurement thus requires an interference with the SM in the $\mu \to e\nu_\mu\bar{\nu}_e$ decay. If this comes from negative interference with a W' this implies $m_{W'} \simeq 1.2\,\text{TeV}$ for $g' = g$ but opposite sign of the couplings to either the muon or electron coupling, compared to the ones for the SM W. The numerical value in eq. (2.12) assumes that the NP that contributes to Γ_μ does not affect any other observables, which is not true for heavy new physics that matches onto SMEFT. We therefore perform a global fit taking all such correlations between different electroweak observables into account.

Assuming that the NP resides only in the $[c_{\ell\ell}]_{1221}$ operator and setting all other Wilson coefficients to zero, the fit to the electroweak observables gives

$$[c_{\ell\ell}]_{1221} = (3.2 \pm 0.6) \times 10^{-3}\,, \tag{2.13}$$

corresponding to

$$m_W = (80.390 \pm 0.006)\,\text{GeV}\,. \tag{2.14}$$

and $\chi^2_{\rm SM} - \min(\chi^2) = 25.9$, which is a significant improvement. However, the goodness of fit is still relatively poor $\chi^2/\text{d.o.f.} = 73.4/(42-1)$. This can be traced to the fact that the change in Γ_μ cannot explain fully the CDF m_W measurement, since the change in the extracted electroweak vacuum expectation value, δv, also feeds in to many of the electroweak observables. This is illustrated in figure 1, where the black solid line denotes the predicted shift in m_W as a function of $1/\Lambda^2 \equiv [c_{\ell\ell}]_{1221}/v^2$. The 1σ best fit band for $[c_{\ell\ell}]_{1221}$ is shown as an orange band. We see that a nonzero $[c_{\ell\ell}]_{1221}$ can increase m_W somewhat above the SM prediction (green), even to the upper range of the PDG average of $m_W^{\rm PDG}$ measurements (blue) which does not yet contain the CDF measurement. It cannot, however, give a shift fully consistent with the CDF measurement (red band). For convenience, we also show the naive average of LEP, ATLAS, LHCb and the new CDF measurement for m_W (magenta), where the errors were inflated according to the PDG prescription, giving $m_W^{\rm inf} = (80.414 \pm 0.018)\,\text{GeV}$.

2.2 New physics modifying the extraction of the electroweak VEV

To capture the effects of other types of new physics that can modify the determination of the electroweak VEV, we perform a fit including all Wilson coefficients entering δv,

JHEP05(2022)133

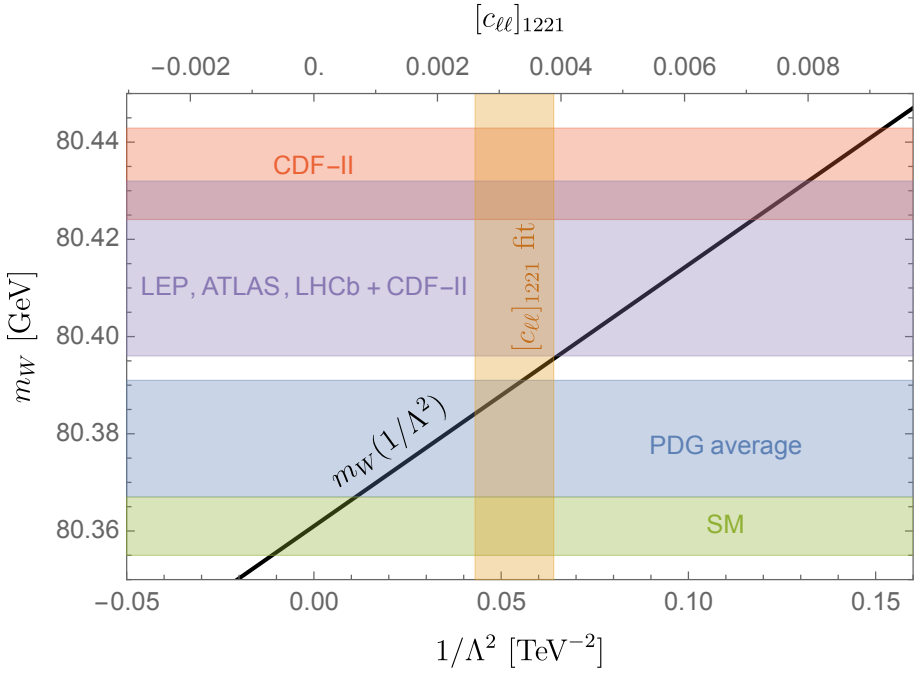

Figure 1. The results of an electroweak fit, where only $1/\Lambda^2 = [c_{\ell\ell}]_{1221}/v^2$ is allowed to be nonzero (orange band). The horizontal bands show the 1σ range of m_W measurement: the PDG average (blue), the recent CDF measurement (red), and our naive average of the two (magenta), along with the prediction of the SM electroweak fit (green). The black line shows the dependence of m_W on $1/\Lambda^2$.

cf. eq. (2.6), while setting the remaining Wilson coefficients in the SMEFT Lagrangian to zero. This yields

$$\begin{pmatrix} [c_{\ell\ell}]_{1221} \\ [c'_{H\ell}]_{11} \\ [c'_{H\ell}]_{22} \end{pmatrix} = \begin{pmatrix} -0.9 \pm 1.8 \\ -1.1 \pm 0.4 \\ -1.4 \pm 0.7 \end{pmatrix} \times 10^{-3}\,, \qquad \rho = \begin{pmatrix} 1 & 0.48 & 0.89 \\ 0.48 & 1 & 0.25 \\ 0.89 & 0.25 & 1 \end{pmatrix}\,, \tag{2.15}$$

with a minimum $\chi^2 = 63.8$ and a prediction for the W mass of $m_W = (80.396 \pm 0.006)$ GeV. That is, if all three parameters entering δv are allowed to vary in the fit, the $[c_{\ell\ell}]_{1221}$ is found to be consistent with zero, and the shift in m_W is due to $[c'_{H\ell}]_{ii}$.

2.3 A fit to the S and T parameters

The oblique parameters S and T encode NP contributions via gauge-boson vacuum-polarization corrections [41]. We assume at the scale m_Z the only non-negligible coefficients are given by c_{WB} and c_T in alignment with many NP models. In the Warsaw basis the coefficients c_{WB} and c_T are related to S and T (assuming $U = 0$) via the relations, see, e.g. [33, 42]

$$c_{WB} = \frac{1}{16\pi} S, \qquad c_T = \frac{g_L^2 g_Y^2}{8\pi(g_Y^2 + g_L^2)} T. \tag{2.16}$$

JHEP05(2022)133

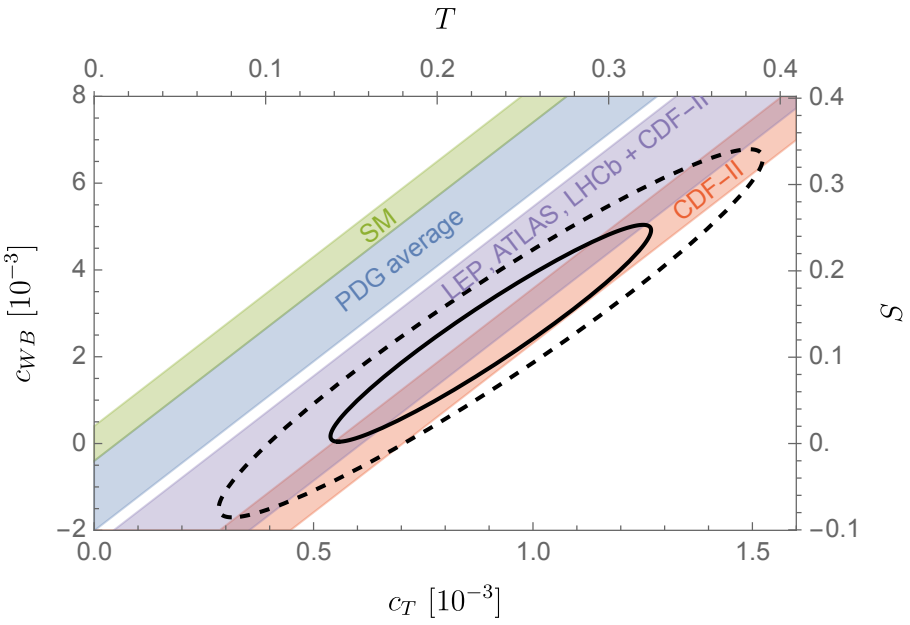

Figure 2. The fit results for coefficients c_T and c_{WB} along with expectation bands for different m_W measurements: SM (green), PDG average (blue), naive average (purple), and the new results from CDF (red). The 1σ (solid) and 2σ (dashed) contours indicate the values from the fit.

By fitting in the two-dimensional space we find

$$c_{WB} = (2.5 \pm 1.6) \times 10^{-3}\,, \qquad c_T = (9 \pm 2) \times 10^{-4}\,, \tag{2.17}$$

with a correlation coefficient $\rho = 0.95$ and the minimum $\chi^2 = 42.8$, and thus the goodness of fit $\chi^2/\text{d.o.f.} = 42.8/(42-2)$ in line with expectations for a valid description of data. The corresponding W mass is $m_W = (80.428 \pm 0.009)\,\text{GeV}$. The above values of c_{WB}, c_T translate to

$$S = 0.13 \pm 0.08, \qquad T = 0.23 \pm 0.05, \tag{2.18}$$

in agreement with current constraints on the S parameter from $h \to \gamma\gamma$ [42]. In figure 2 we show the results of our fit including estimated S and T values.

2.4 A global flavorful fit

Finally, we vary all the Z and W couplings to preform a global flavorful fit, following refs. [32, 33]. In particular, this fit also allows for generational dependence of W and Z couplings to the SM fermions. We quote the results in terms of the modified Wilson

JHEP05(2022)133

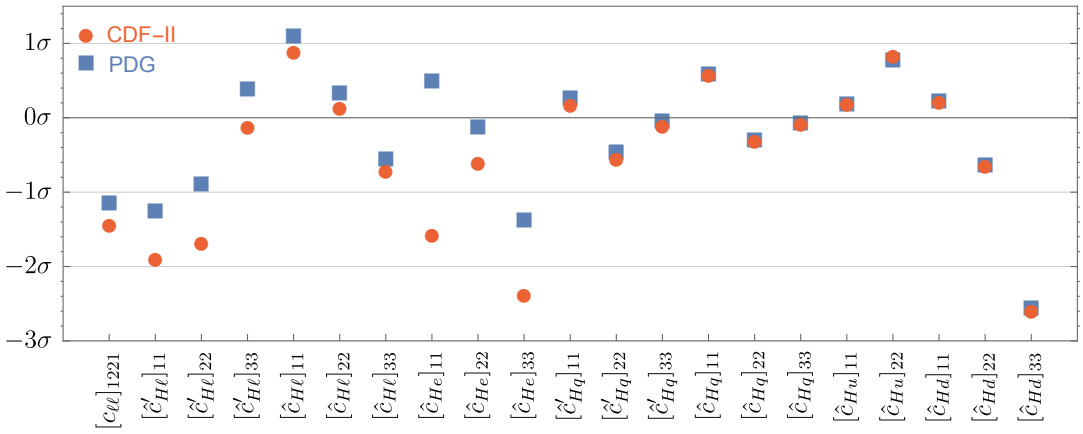

Figure 3. Pulls of the flavorful fit results using the CDF-II measurement of the W mass (red dots) and PDG average (blue rectangles).

coefficients in the Warsaw basis, see appendix A of [32],

$$
\begin{aligned}
[c_{\ell\ell}]_{1221} &= (-1.31 \pm 0.90) \times 10^{-2}\,, \\
[\hat{c}'_{H\ell}]_{ii} &= \begin{pmatrix} -0.62 \pm 0.32 \\ -0.45 \pm 0.26 \\ -0.06 \pm 0.41 \end{pmatrix} \times 10^{-2}\,, \qquad [\hat{c}_{H\ell}]_{ii} = \begin{pmatrix} 0.27 \pm 0.31 \\ 0.04 \pm 0.34 \\ -0.31 \pm 0.42 \end{pmatrix} \times 10^{-2}\,, \\
[\hat{c}_{He}]_{ii} &= \begin{pmatrix} -0.09 \pm 0.06 \\ -0.17 \pm 0.27 \\ -0.30 \pm 0.13 \end{pmatrix} \times 10^{-2}\,, \\
[\hat{c}'_{Hq}]_{ii} &= \begin{pmatrix} 0.41 \pm 2.67 \\ -1.58 \pm 2.78 \\ -0.49 \pm 4.10 \end{pmatrix} \times 10^{-2}\,, \qquad [\hat{c}_{Hq}]_{ii} = \begin{pmatrix} 3.08 \pm 5.49 \\ -0.91 \pm 2.83 \\ -0.42 \pm 4.11 \end{pmatrix} \times 10^{-2}\,, \\
[\hat{c}_{Hu}]_{ii} &= \begin{pmatrix} 1.05 \pm 6.27 \\ 0.84 \pm 1.04 \\ — \end{pmatrix} \times 10^{-2}\,, \qquad [\hat{c}_{Hd}]_{ii} = \begin{pmatrix} 5.07 \pm 25.84 \\ -6.46 \pm 9.68 \\ -4.54 \pm 1.74 \end{pmatrix} \times 10^{-2}\,.
\end{aligned}
\tag{2.19}
$$

This corresponds to a $\chi^2 = 26.6$ and a W mass of $m_W = (80.434 \pm 0.009)\,\text{GeV}$ at the best-fit point. The goodness of fit $\chi^2/\text{d.o.f.} = 26.6/(42-21)$ is in fact better than one would naively expect.

The pulls for the values of the modified Wilson coefficients (2.19) are plotted in figure 3 (red dots), where we compare them to the pulls that are obtained from a global fit in which the only change in the inputs is the use of the PDG average for the W mass, m_W^{PDG}, see also section A. Note that there is no single operator that exhibits a 3σ evidence for a nonzero value, both within the electroweak fit with the PDG as well as in the fit with the CDF value of m_W. A comparison of the two fit results shows that there are a number of effective

JHEP05(2022)133

Wilson coefficients in which the evidence for nonzero value strengthened. Most notably, these are the effective Wilson coefficients that contribute to δv, the coefficients $[c_{\ell\ell}]_{1221}$, $[\hat{c}'_{H\ell}]_{11}$, $[\hat{c}'_{H\ell}]_{22}$, where

$$[\hat{c}'_{H\ell}]_{ij} = [c'_{H\ell}]_{ij} + \delta_{ij}\left(g_L^2 c_{WB} - \frac{g_L^2}{g_Y^2} c_T\right). \tag{2.20}$$

The flavor universal part is given by a linear combination of S and T parameters, while the fit suggests also nonzero flavor non-universal contributions. A large change in the pull is also observed in the effective Wilson coefficient $[\hat{c}_{He}]_{11}$ and $[\hat{c}_{He}]_{33}$, where

$$[\hat{c}_{He}]_{ij} = [c_{He}]_{ij} - 2c_T\delta_{ij}, \tag{2.21}$$

Also in this case the data shows preference for nonvanishing flavor non-universal contributions.

3 Models

3.1 Tree level contributions to δv

The two models that can lead to a tree level contribution to $[c_{\ell\ell}]_{1221}$ are the W' mediator and the S_1 scalar mediator, which we discuss in turn.

The W' with effective interactions. A heavy vector boson, W'^a_μ, a triplet of $\mathrm{SU}(2)_L$, can have the following effective interactions with the leptons

$$\mathcal{L}_{W'} \supset \frac{1}{2} W'^a_\mu \left(g_H H^\dagger \sigma^a i \overleftrightarrow{D}_\mu H + g_{\ell_i} \bar{\ell}_i \sigma^a \gamma_\mu \ell_i + \cdots\right). \tag{3.1}$$

Integrating out the W' gives

$$[c_{\ell\ell}]_{1221} = -\frac{g_{\ell_1} g_{\ell_2}}{2} \frac{v^2}{m_{W'}^2} = 3 \times 10^{-3} \times (-g_{\ell_1} g_{\ell_2}) \left(\frac{3.1\,\mathrm{TeV}}{m_{W'}}\right)^2, \tag{3.2}$$

$$[c'_{H\ell}]_{ii} = -\frac{g_H g_{\ell_i}}{4 m_{W'}^2} = -10^{-3} \times (g_H g_{\ell_i}) \left(\frac{3.9\,\mathrm{TeV}}{m_{W'}}\right)^2, \tag{3.3}$$

where $m_{W'}$ is the W' mass. In the numerical examples on the r.h.s. we used the values close to the central values of the fits in sections 2.1 and 2.2. If the shift in m_W is explained by just new physics in $[c_{\ell\ell}]_{1221}$ this needs to be positive, see section 2.1, which would mean that the W' needs to couple to the first and the second generation fermions with the opposite sign. Since the couplings of the new vector boson are then flavor non-universal, this is not easy to achieve in a complete UV model, while satisfying all the flavor constraints. In contrast, when all three operators are allowed to be varied in the fit, the main contribution is found to arise from $[c'_{H\ell}]_{ii}$, see section 2.2. The pattern in the data can thus be matched if g_H is larger than g_{ℓ_i}.

JHEP05(2022)133

Tree level contribution from charged scalar. The scalar S_1 that carries a hypercharge 1 has couplings to lepton doublets of the form [43]

$$\mathcal{L}_{S_1} \supset y_{ij} S_1 \bar{\ell}_{Li} i\sigma_2 \ell^c_{Lj} + \text{h.c.}. \tag{3.4}$$

Integrating out the scalar generates the $[c_{\ell\ell}]_{1221}$ from the couplings to the first two generations

$$[c_{\ell\ell}]_{1221} = -\frac{y_{12} y_{12}^*}{2} \frac{v^2}{m_{S_1}^2}. \tag{3.5}$$

3.2 Top-partners

Naturalness demands that the quadratic divergence of the one-loop top contribution to the Higgs mass is cancelled at roughly the TeV scale. In many of the known extensions of the SM this is achieved, mechanically, by adding top partners, scalars or fermions, weak-singlets and doublets with order one Yukawa couplings to the SM top sector (see for instance ref. [44] for a more detailed discussion). Here we focus on the question whether fermionic, spin-1/2, top partners can give rise to the relevant shifts in the oblique parameters found in eq. (2.17), such that the CDF measurement of the W mass is explained, and set aside the precise details of the full UV model. For concreteness we consider the minimal content, adding either a single vector-like top-singlet partner or a vector-like third-generation doublet partner. In figure 4 we show the one and two sigma CL contours for the singlet and doublet partners where on the vertical axis we show the mixing-angle as a function of the partner mass. In partner models we expect that the mixing angle is of the order of $v/\sqrt{2}m_T$, with m_T the partner mass (for simplicity, we consider a single mass and a single mixing angle, in the heavy mass limit as required by the LHC limits [45], for a complete description of the dependencies see, e.g., ref. [46]). We find that models with such spin-1/2 partners can account for the observed shift in the W mass, with an order one Yukawa, for a broad range of parameter space for TeV partner-masses.

4 Conclusions

While tension between the CDF legacy measurement of the W mass and the global average of m_W determinations may give one pause, intriguingly, the CDF value of m_W does lend itself to a number of new physics explanations. In this paper, we performed several different fits to electroweak observable data. The best description of the data is obtained with a global flavorful fit, where preference for flavor non-universality is indicated by the data. A subset of operators can also give a reasonable description of the data, most notably a fit that assumes the new physics resides mainly in the oblique parameters. The new physics contributions that affect the extraction of the electroweak VEV, such as the change in muon lifetime, on the other hand, while improving the quality of the fit compared to the SM, cannot explain the entire tension between the CDF m_W measurement and the SM prediction. Finally, we point out that top partners with order TeV masses could lead to the observed shift in the W mass.

JHEP05(2022)133

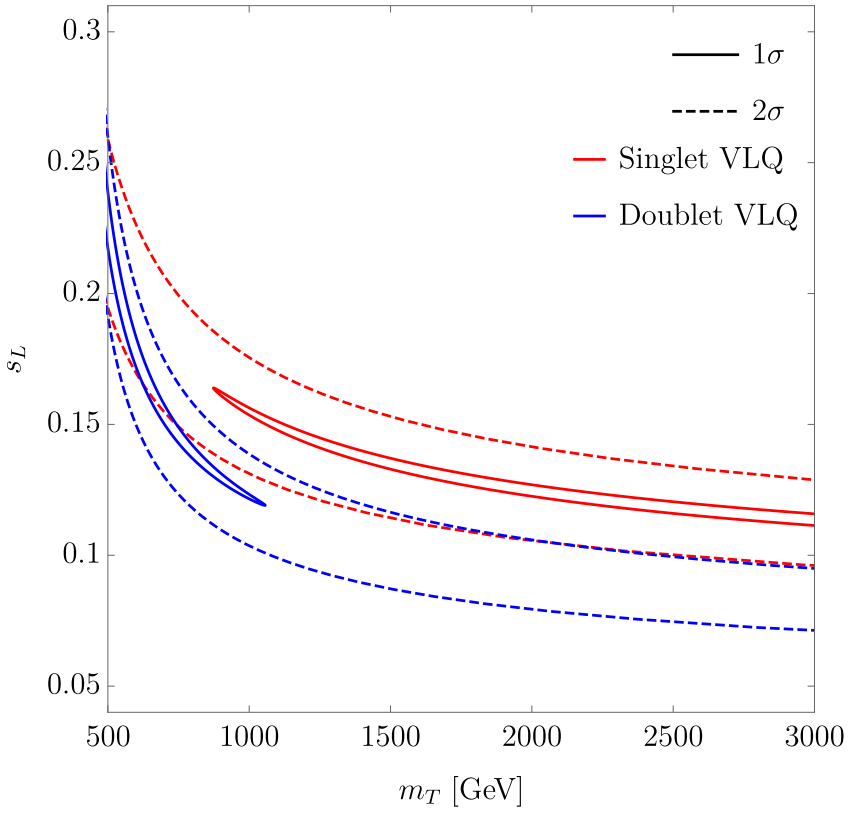

Figure 4. The one (solid) and two (dashed) sigma CL contours for the singlet (red) and doublet (blue) partners where on the vertical axis we show the mixing-angle as a function of the vector-like (VLQ) quark mass, see text for more details.

Acknowledgments

We thank Yael Shadmi for useful discussions. The work of RB and YS is supported by grants from the NSF-BSF (No. 2018683), the ISF (No. 482/20), the BSF (No. 2020300) and by the Azrieli foundation. The work of EM is supported by the Minerva Foundation. TM and JZ acknowledge support in part by the DOE grant de-sc0011784. The work of GP is supported by grants from BSF-NSF (No. 2019760), Friedrich Wilhelm Bessel research award, GIF, the ISF (grant No. 718/18), Minerva, SABRA-Yeda-Sela-WRC Program, the Estate of Emile Mimran, and The Maurice and Vivienne Wohl Endowment.

A Fit with $m_W^{\rm PDG}$

In this appendix we collect the numerical results of the full flavorful fit, which in contrast to the results in the main text uses the PDG value of the W mass, $m_W^{\rm PDG}$ (and not $m_W^{\rm CDF}$),

JHEP05(2022)133

while all the remaining inputs are the same. This gives for the modified Wilson coefficients

$$
\begin{aligned}
[c_{\ell\ell}]_{1221} &= (-1.07 \pm 0.91) \times 10^{-2}\,, \\
[\hat{c}'_{H\ell}]_{ii} &= \begin{pmatrix} -0.42 \pm 0.33 \\ -0.25 \pm 0.27 \\ 0.14 \pm 0.41 \end{pmatrix} \times 10^{-2}\,, \qquad [\hat{c}_{H\ell}]_{ii} = \begin{pmatrix} 0.33 \pm 0.31 \\ 0.1 \pm 0.34 \\ -0.25 \pm 0.42 \end{pmatrix} \times 10^{-2}\,, \\
[\hat{c}_{He}]_{ii} &= \begin{pmatrix} 0.03 \pm 0.06 \\ -0.04 \pm 0.27 \\ -0.18 \pm 0.13 \end{pmatrix} \times 10^{-2}\,, \\
[\hat{c}'_{Hq}]_{ii} &= \begin{pmatrix} 0.61 \pm 2.67 \\ -1.38 \pm 2.78 \\ -0.29 \pm 4.10 \end{pmatrix} \times 10^{-2}\,, \qquad [\hat{c}_{Hq}]_{ii} = \begin{pmatrix} 3.06 \pm 5.49 \\ -0.94 \pm 2.83 \\ -0.44 \pm 4.11 \end{pmatrix} \times 10^{-2}\,, \\
[\hat{c}_{Hu}]_{ii} &= \begin{pmatrix} 0.97 \pm 6.27 \\ 0.76 \pm 1.04 \\ — \end{pmatrix} \times 10^{-2}\,, \qquad [\hat{c}_{Hd}]_{ii} = \begin{pmatrix} 5.11 \pm 25.84 \\ -6.42 \pm 9.68 \\ -4.5 \pm 1.74 \end{pmatrix} \times 10^{-2}\,.
\end{aligned}
\tag{A.1}
$$

The fit yields $\chi^2/\text{d.o.f.} = 26.6/(42-21)$ with $\Delta\chi^2 = 17$ compared to the pure SM without dimension six contributions. The corresponding prediction for the W mass is $m_W = (80.379 \pm 0.012)\,\text{GeV}$.

B Inputs and correlation matrices

The inputs used in the global fit are given in table 1. We also list the two correlation matrices, for the fit using the CDF value of m_W, and for the fit using the PDG value. The correlation matrix for the CDF fit can be found in eq. (B.1). The correlation matrix following from the fit using the PDG average for the W mass is given in eq. (B.2). The rows and columns correspond to the 21 effective Wilson coefficients ($[c_{\ell\ell}]_{1221}$, $[\hat{c}'_{H\ell}]_{11}$, $[\hat{c}'_{H\ell}]_{22}$, $[\hat{c}'_{H\ell}]_{33}$, $[\hat{c}_{H\ell}]_{11}$, $[\hat{c}_{H\ell}]_{22}$, $[\hat{c}_{H\ell}]_{33}$, $[\hat{c}_{He}]_{11}$, $[\hat{c}_{He}]_{22}$, $[\hat{c}_{He}]_{33}$, $[\hat{c}'_{Hq}]_{11}$, $[\hat{c}'_{Hq}]_{22}$, $[\hat{c}'_{Hq}]_{33}$, $[\hat{c}_{Hq}]_{11}$, $[\hat{c}_{Hq}]_{22}$, $[\hat{c}_{Hq}]_{33}$, $[\hat{c}_{Hu}]_{11}$, $[\hat{c}_{Hu}]_{22}$, $[\hat{c}_{Hd}]_{11}$, $[\hat{c}_{Hd}]_{22}$, $[\hat{c}_{Hd}]_{33}$), where for simplicity we neglected the flavor off-diagonal components in the fit.

JHEP05(2022)133

Observable	Experimental value	SM value	Ref.	Observable	Experimental value	SM value	Ref.
m_Z	(91.1876 ± 0.0021) GeV	91.1882 GeV	[5]	m_W	(80.4335 ± 0.0094) GeV	80.361 GeV	[1]
Γ_Z	(2.4955 ± 0.0023) GeV	2.4941 GeV	[47, 48]	Γ_W	(2.085 ± 0.042) GeV	2.088 GeV	[5]
σ_{had}	(41.4802 ± 0.0325) nb	41.4842 nb	[47, 48]	$\text{Br}\,(W \to e\nu)$	0.1071 ± 0.0016	0.1082	[2]
R_e	20.804 ± 0.050	20.734	[47]	$\text{Br}\,(W \to \mu\nu)$	0.1063 ± 0.0015	0.1082	[2]
R_μ	20.785 ± 0.033	20.734	[47]	$\text{Br}\,(W \to \tau\nu)$	0.1138 ± 0.0021	0.1081	[2]
R_τ	20.764 ± 0.045	20.781	[47]	$\frac{\text{Br}(W\to\mu\nu)}{\text{Br}(W\to e\nu)}$	0.982 ± 0.024	1	[49]
$A_{\text{FB}}^{0,e}$	0.0145 ± 0.0025	0.0162	[47]		1.020 ± 0.019		[50]
$A_{\text{FB}}^{0,\mu}$	0.0169 ± 0.0013	0.0162	[47]		1.003 ± 0.010		[51]
$A_{\text{FB}}^{0,\tau}$	0.0188 ± 0.0017	0.0162	[47]	$\frac{\text{Br}(W\to\tau\nu)}{\text{Br}(W\to e\nu)}$	0.961 ± 0.061	0.999	[5, 52]
R_b	$0.216\,29 \pm 0.000\,66$	0.215 81	[47]	$\frac{\text{Br}(W\to\tau\nu)}{\text{Br}(W\to\mu\nu)}$	0.992 ± 0.013	0.999	[53]
R_c	0.1721 ± 0.0030	0.172 22	[47]	R_{Wc}	0.49 ± 0.04	0.50	[5]
$A_{\text{FB}}^{0,b}$	0.0996 ± 0.0016	0.1032	[47, 54]	R_σ	0.998 ± 0.041	1	[55]
$A_{\text{FB}}^{0,c}$	0.0707 ± 0.0035	0.0736	[47]	$g_{u,A}^{\text{D0}}$	0.501 ± 0.110	0.501	[56]
A_e	0.1516 ± 0.0021	0.1470	[47]	$g_{u,V}^{\text{D0}}$	0.201 ± 0.112	0.192	[56]
	0.1498 ± 0.0049		[47]	$g_{d,A}^{\text{D0}}$	-0.497 ± 0.165	-0.502	[56]
A_μ	0.142 ± 0.015	0.1470	[47]	$g_{d,V}^{\text{D0}}$	-0.351 ± 0.251	-0.347	[56]
A_τ	0.136 ± 0.015	0.1470	[47]	$A_4(0 \le \lvert Y\rvert < 0.8)$	0.0195 ± 0.0015	0.0144	[34, 57]
	0.1439 ± 0.0043		[47]	$A_4(0.8 \le \lvert Y\rvert < 1.6)$	0.0448 ± 0.0016	0.0471	[34, 57]
A_b	0.923 ± 0.020	0.935	[47]	$A_4(1.6 \le \lvert Y\rvert < 2.5)$	0.0923 ± 0.0026	0.0928	[34, 57]
A_c	0.670 ± 0.027	0.668	[47]	$A_4(2.5 \le \lvert Y\rvert < 3.2)$	0.1445 ± 0.0046	0.1464	[34, 57]
A_s	0.895 ± 0.091	0.936	[58]	R_{uc}	0.166 ± 0.009	0.1722	[5]

Table 1. Observables used in the fit.

JHEP05(2022)133

$$\rho^{\mathrm{CDF}} = \begin{pmatrix}
100 & 82 & 71 & -64 & -78 & -47 & 62 & -19 & 19 & 13 & 1 & 3 & 0 & 5 & 3 & -1 & 7 & -1 & 8 & 5 & -1 \\
82 & 100 & 21 & -57 & -97 & -8 & 56 & -10 & 14 & 10 & 1 & 3 & 0 & 4 & 3 & 0 & 5 & -1 & 6 & 4 & -1 \\
71 & 21 & 100 & -37 & -14 & -69 & 37 & -12 & 17 & 13 & 1 & 3 & 0 & 4 & 3 & 0 & 6 & -1 & 7 & 4 & -1 \\
-64 & -57 & -37 & 100 & 64 & 36 & -95 & -8 & 11 & 8 & 0 & 0 & 0 & 0 & 0 & 0 & 0 & 0 & 0 & 0 & -1 \\
-78 & -97 & -14 & 64 & 100 & 4 & -61 & 19 & -14 & -7 & 0 & -2 & 0 & -3 & -2 & 0 & -5 & 2 & -5 & -3 & -5 \\
-47 & -8 & -69 & 36 & 4 & 100 & -32 & 13 & 53 & -10 & 0 & -1 & 0 & -3 & -2 & 1 & -4 & 0 & -5 & -3 & 3 \\
62 & 56 & 37 & -95 & -61 & -32 & 100 & 13 & -11 & 5 & 0 & 1 & 0 & 0 & 0 & 0 & 0 & 0 & 0 & 0 & 1 \\
-19 & -10 & -12 & -8 & 19 & 13 & 13 & 100 & -3 & 4 & 0 & -1 & 0 & -2 & 0 & -3 & -2 & 10 & -3 & -2 & -35 \\
19 & 14 & 17 & 11 & -14 & 53 & -11 & -3 & 100 & 5 & 0 & 1 & 0 & 2 & 1 & 0 & 3 & -2 & 3 & 2 & 3 \\
13 & 10 & 13 & 8 & -7 & -10 & 5 & 4 & 5 & 100 & 0 & 1 & 0 & 2 & 1 & 0 & 2 & -1 & 3 & 2 & 0 \\
1 & 1 & 1 & 0 & 0 & 0 & 0 & 0 & 0 & 0 & 100 & -94 & 0 & 53 & -92 & 0 & 32 & -1 & 14 & 14 & 0 \\
3 & 3 & 3 & 0 & -2 & -1 & 1 & -1 & 1 & 1 & -94 & 100 & 0 & -39 & 98 & 0 & -12 & -1 & 7 & -1 & 0 \\
0 & 0 & 0 & 0 & 0 & 0 & 0 & 0 & 0 & 0 & 0 & 0 & 100 & 0 & 0 & -100 & 0 & 0 & 0 & 0 & 0 \\
5 & 4 & 4 & 0 & -3 & -3 & 0 & -2 & 2 & 2 & 53 & -39 & 0 & 100 & -39 & 0 & 58 & 7 & 65 & -18 & -1 \\
3 & 3 & 3 & 0 & -2 & -2 & 0 & 0 & 1 & 1 & -92 & 98 & 0 & -39 & 100 & 0 & -10 & 8 & 8 & 0 & -3 \\
-1 & 0 & 0 & 0 & 0 & 1 & 0 & -3 & 0 & 0 & 0 & 0 & -100 & 0 & 0 & 100 & 0 & -1 & 0 & 0 & 7 \\
7 & 5 & 6 & 0 & -5 & -4 & 0 & -2 & 3 & 2 & 32 & -12 & 0 & 58 & -10 & 0 & 100 & 7 & 95 & -39 & -2 \\
-1 & -1 & -1 & 0 & 2 & 0 & 0 & 10 & -2 & -1 & -1 & -1 & 0 & 7 & 8 & -1 & 7 & 100 & 9 & 5 & -16 \\
8 & 6 & 7 & 0 & -5 & -5 & 0 & -3 & 3 & 3 & 14 & 7 & 0 & 65 & 8 & 0 & 95 & 9 & 100 & -46 & -2 \\
5 & 4 & 4 & 0 & -3 & -3 & 0 & -2 & 2 & 2 & 14 & -1 & 0 & -18 & 0 & 0 & -39 & 5 & -46 & 100 & -1 \\
-1 & -1 & -1 & -1 & -5 & 3 & 1 & -35 & 3 & 0 & 0 & 0 & 0 & -1 & -3 & 7 & -2 & -16 & -2 & -1 & 100
\end{pmatrix} \times 10^{-2} \quad \text{(B.1)}$$

$$\rho^{\mathrm{PDG}} = \begin{pmatrix}
100 & 82 & 71 & -63 & -78 & -46 & 62 & -17 & 19 & 13 & 1 & 3 & 0 & 5 & 3 & -1 & 7 & -1 & 8 & 5 & -1 \\
82 & 100 & 21 & -56 & -97 & -8 & 56 & -7 & 14 & 11 & 1 & 3 & 0 & 4 & 3 & 0 & 5 & -1 & 6 & 4 & -1 \\
71 & 21 & 100 & -36 & -14 & -68 & 37 & -8 & 18 & 14 & 1 & 3 & 0 & 4 & 3 & 0 & 6 & -1 & 7 & 4 & -1 \\
-63 & -56 & -36 & 100 & 64 & 36 & -95 & -6 & 12 & 9 & 0 & 0 & 0 & 0 & 0 & 0 & 0 & 0 & 0 & 0 & -1 \\
-78 & -97 & -14 & 64 & 100 & 4 & -61 & 19 & -13 & -6 & 0 & -2 & 0 & -3 & -2 & 0 & -5 & 2 & -5 & -3 & -5 \\
-46 & -8 & -68 & 36 & 4 & 100 & -32 & 13 & 53 & -9 & 0 & -1 & 0 & -3 & -2 & 1 & -4 & 0 & -5 & -3 & 4 \\
62 & 56 & 37 & -95 & -61 & -32 & 100 & 13 & -11 & 6 & 0 & 1 & 0 & 0 & 0 & 0 & 0 & 0 & 0 & 0 & 1 \\
-17 & -7 & -8 & -6 & 19 & 13 & 13 & 100 & 0 & 8 & 1 & -1 & 1 & -2 & 0 & -3 & -2 & 9 & -2 & -2 & -33 \\
19 & 14 & 18 & 12 & -13 & 53 & -11 & 0 & 100 & 6 & 0 & 1 & 0 & 2 & 1 & 0 & 3 & -2 & 3 & 2 & 3 \\
13 & 11 & 14 & 9 & -6 & -9 & 6 & 8 & 6 & 100 & 0 & 1 & 0 & 2 & 1 & 0 & 2 & -1 & 3 & 2 & 0 \\
1 & 1 & 1 & 0 & 0 & 0 & 0 & 1 & 0 & 0 & 100 & -94 & 0 & 53 & -92 & 0 & 32 & -1 & 14 & 14 & 0 \\
3 & 3 & 3 & 0 & -2 & -1 & 1 & -1 & 1 & 1 & -94 & 100 & 0 & -39 & 98 & 0 & -12 & -1 & 7 & -1 & 0 \\
0 & 0 & 0 & 0 & 0 & 0 & 0 & 1 & 0 & 0 & 0 & 0 & 100 & 0 & 0 & -100 & 0 & 0 & 0 & 0 & 0 \\
5 & 4 & 4 & 0 & -3 & -3 & 0 & -2 & 2 & 2 & 53 & -39 & 0 & 100 & -39 & 0 & 58 & 7 & 65 & -18 & -1 \\
3 & 3 & 3 & 0 & -2 & -2 & 0 & 0 & 1 & 1 & -92 & 98 & 0 & -39 & 100 & 0 & -10 & 8 & 8 & 0 & -3 \\
-1 & 0 & 0 & 0 & 0 & 1 & 0 & -3 & 0 & 0 & 0 & 0 & -100 & 0 & 0 & 100 & 0 & -1 & 0 & 0 & 7 \\
7 & 5 & 6 & 0 & -5 & -4 & 0 & -2 & 3 & 2 & 32 & -12 & 0 & 58 & -10 & 0 & 100 & 7 & 95 & -39 & -2 \\
-1 & -1 & -1 & 0 & 2 & 0 & 0 & 9 & -2 & -1 & -1 & -1 & 0 & 7 & 8 & -1 & 7 & 100 & 9 & 5 & -16 \\
8 & 6 & 7 & 0 & -5 & -5 & 0 & -2 & 3 & 3 & 14 & 7 & 0 & 65 & 8 & 0 & 95 & 9 & 100 & -46 & -2 \\
5 & 4 & 4 & 0 & -3 & -3 & 0 & -2 & 2 & 2 & 14 & -1 & 0 & -18 & 0 & 0 & -39 & 5 & -46 & 100 & -1 \\
-1 & -1 & -1 & -1 & -5 & 4 & 1 & -33 & 3 & 0 & 0 & 0 & 0 & -1 & -3 & 7 & -2 & -16 & -2 & -1 & 100
\end{pmatrix} \times 10^{-2} \quad \text{(B.2)}$$

JHEP05(2022)133

References

[1] CDF collaboration, *High-precision measurement of the W boson mass with the CDF II detector*, *Science* **376** (2022) 170 [INSPIRE].

[2] ALEPH, DELPHI, L3, OPAL and LEP Electroweak collaborations, *Electroweak measurements in electron-positron collisions at W-boson-pair energies at LEP*, *Phys. Rept.* **532** (2013) 119 [arXiv:1302.3415] [INSPIRE].

[3] ATLAS collaboration, *Measurement of the W-boson mass in pp collisions at $\sqrt{s} = 7$ TeV with the ATLAS detector*, *Eur. Phys. J. C* **78** (2018) 110 [*Erratum ibid.* **78** (2018) 898] [arXiv:1701.07240] [INSPIRE].

[4] CDF and D0 collaborations, *Combination of CDF and D0 W-boson mass measurements*, *Phys. Rev. D* **88** (2013) 052018 [arXiv:1307.7627] [INSPIRE].

[5] Particle Data Group collaboration, *Review of particle physics*, *PTEP* **2020** (2020) 083C01 [INSPIRE].

[6] LHCb collaboration, *Measurement of the W boson mass*, *JHEP* **01** (2022) 036 [arXiv:2109.01113] [INSPIRE].

[7] C.-T. Lu, L. Wu, Y. Wu and B. Zhu, *Electroweak precision fit and new physics in light of W boson mass*, arXiv:2204.03796 [INSPIRE].

[8] A. Strumia, *Interpreting electroweak precision data including the W-mass CDF anomaly*, arXiv:2204.04191 [INSPIRE].

[9] J. de Blas, M. Pierini, L. Reina and L. Silvestrini, *Impact of the recent measurements of the top-quark and W-boson masses on electroweak precision fits*, arXiv:2204.04204 [INSPIRE].

[10] J. Fan, L. Li, T. Liu and K.-F. Lyu, *W-boson mass, electroweak precision tests and SMEFT*, arXiv:2204.04805 [INSPIRE].

[11] T.-P. Tang, M. Abdughani, L. Feng, Y.-L.S. Tsai and Y.-Z. Fan, *NMSSM neutralino dark matter for W-boson mass and muon $g-2$ and the promising prospect of direct detection*, arXiv:2204.04356 [INSPIRE].

[12] G. Cacciapaglia and F. Sannino, *The W boson mass weighs in on the non-standard Higgs*, arXiv:2204.04514 [INSPIRE].

[13] M. Blennow, P. Coloma, E. Fernández-Martínez and M. González-López, *Right-handed neutrinos and the CDF II anomaly*, arXiv:2204.04559 [INSPIRE].

[14] X. Liu, S.-Y. Guo, B. Zhu and Y. Li, *Unifying gravitational waves with W boson, FIMP dark matter, and Majorana seesaw mechanism*, arXiv:2204.04834 [INSPIRE].

[15] H.M. Lee and K. Yamashita, *A model of vector-like leptons for the muon $g-2$ and the W boson mass*, arXiv:2204.05024 [INSPIRE].

[16] Y. Cheng, X.-G. He, Z.-L. Huang and M.-W. Li, *Type-II seesaw triplet scalar and its VEV effects on neutrino trident scattering and W mass*, arXiv:2204.05031 [INSPIRE].

JHEP05(2022)133

[17] H. Song, W. Su and M. Zhang, *Electroweak phase transition in 2HDM under Higgs, Z-pole, and W precision measurements*, arXiv:2204.05085 [INSPIRE].

[18] E. Bagnaschi, J. Ellis, M. Madigan, K. Mimasu, V. Sanz and T. You, *SMEFT analysis of m_W*, arXiv:2204.05260 [INSPIRE].

[19] A. Paul and M. Valli, *Violation of custodial symmetry from W-boson mass measurements*, arXiv:2204.05267 [INSPIRE].

[20] H. Bahl, J. Braathen and G. Weiglein, *New physics effects on the W-boson mass from a doublet extension of the SM Higgs sector*, arXiv:2204.05269 [INSPIRE].

[21] P. Asadi, C. Cesarotti, K. Fraser, S. Homiller and A. Parikh, *Oblique lessons from the W mass measurement at CDF II*, arXiv:2204.05283 [INSPIRE].

[22] L. Di Luzio, R. Gröber and P. Paradisi, *Higgs physics confronts the M_W anomaly*, arXiv:2204.05284 [INSPIRE].

[23] P. Athron, M. Bach, D.H.J. Jacob, W. Kotlarski, D. Stöckinger and A. Voigt, *Precise calculation of the W boson pole mass beyond the Standard Model with FlexibleSUSY*, arXiv:2204.05285 [INSPIRE].

[24] J. Gu, Z. Liu, T. Ma and J. Shu, *Speculations on the W-mass measurement at CDF*, arXiv:2204.05296 [INSPIRE].

[25] K.S. Babu, S. Jana and V.P. K., *Correlating W-boson mass shift with muon $g-2$ in the 2HDM*, arXiv:2204.05303 [INSPIRE].

[26] F. Arias-Aragón, E. Fernández-Martínez, M. González-López and L. Merlo, *Dynamical minimal flavour violating inverse seesaw*, arXiv:2204.04672 [INSPIRE].

[27] K. Sakurai, F. Takahashi and W. Yin, *Singlet extensions and W boson mass in the light of the CDF II result*, arXiv:2204.04770 [INSPIRE].

[28] P. Athron, A. Fowlie, C.-T. Lu, L. Wu, Y. Wu and B. Zhu, *The W boson mass and muon $g-2$: hadronic uncertainties or new physics?*, arXiv:2204.03996 [INSPIRE].

[29] J.J. Heckman, *Extra W-boson mass from a D3-brane*, arXiv:2204.05302 [INSPIRE].

[30] M. Backović, *A theory of ambulance chasing*, arXiv:1603.01204 [INSPIRE].

[31] A. Falkowski and F. Riva, *Model-independent precision constraints on dimension-6 operators*, *JHEP* **02** (2015) 039 [arXiv:1411.0669] [INSPIRE].

[32] A. Efrati, A. Falkowski and Y. Soreq, *Electroweak constraints on flavorful effective theories*, *JHEP* **07** (2015) 018 [arXiv:1503.07872] [INSPIRE].

[33] A. Falkowski and D. Straub, *Flavourful SMEFT likelihood for Higgs and electroweak data*, *JHEP* **04** (2020) 066 [arXiv:1911.07866] [INSPIRE].

[34] V. Bresó-Pla, A. Falkowski and M. González-Alonso, *A_{FB} in the SMEFT: precision Z physics at the LHC*, *JHEP* **08** (2021) 021 [arXiv:2103.12074] [INSPIRE].

[35] B. Grinstein and M.B. Wise, *Operator analysis for precision electroweak physics*, *Phys. Lett. B* **265** (1991) 326 [INSPIRE].

[36] B. Grzadkowski, M. Iskrzynski, M. Misiak and J. Rosiek, *Dimension-six terms in the Standard Model Lagrangian*, *JHEP* **10** (2010) 085 [arXiv:1008.4884] [INSPIRE].

[37] D. d'Enterria and V. Jacobsen, *Improved strong coupling determinations from hadronic decays of electroweak bosons at N^3LO accuracy*, arXiv:2005.04545 [INSPIRE].

JHEP05(2022)133

[38] M. Awramik, M. Czakon, A. Freitas and G. Weiglein, *Precise prediction for the W boson mass in the Standard Model*, *Phys. Rev. D* **69** (2004) 053006 [hep-ph/0311148] [INSPIRE].

[39] B. Capdevila, A. Crivellin, C.A. Manzari and M. Montull, *Explaining $b \to s\ell^+\ell^-$ and the Cabibbo angle anomaly with a vector triplet*, *Phys. Rev. D* **103** (2021) 015032 [arXiv:2005.13542] [INSPIRE].

[40] A. Crivellin, M. Hoferichter and C.A. Manzari, *Fermi constant from muon decay versus electroweak fits and Cabibbo-Kobayashi-Maskawa unitarity*, *Phys. Rev. Lett.* **127** (2021) 071801 [arXiv:2102.02825] [INSPIRE].

[41] M.E. Peskin and T. Takeuchi, *A new constraint on a strongly interacting Higgs sector*, *Phys. Rev. Lett.* **65** (1990) 964 [INSPIRE].

[42] J. Ellis, C.W. Murphy, V. Sanz and T. You, *Updated global SMEFT fit to Higgs, diboson and electroweak data*, *JHEP* **06** (2018) 146 [arXiv:1803.03252] [INSPIRE].

[43] J. de Blas, J.C. Criado, M. Pérez-Victoria and J. Santiago, *Effective description of general extensions of the Standard Model: the complete tree-level dictionary*, *JHEP* **03** (2018) 109 [arXiv:1711.10391] [INSPIRE].

[44] J. Berger, J. Hubisz and M. Perelstein, *A fermionic top partner: naturalness and the LHC*, *JHEP* **07** (2012) 016 [arXiv:1205.0013] [INSPIRE].

[45] A. Banerjee et al., *Phenomenological aspects of composite Higgs scenarios: exotic scalars and vector-like quarks*, arXiv:2203.07270 [INSPIRE].

[46] C.-Y. Chen, S. Dawson and E. Furlan, *Vectorlike fermions and Higgs effective field theory revisited*, *Phys. Rev. D* **96** (2017) 015006 [arXiv:1703.06134] [INSPIRE].

[47] ALEPH, DELPHI, L3, OPAL, SLD, LEP Electroweak Working Group, SLD Electroweak Group and SLD Heavy Flavour Group collaborations, *Precision electroweak measurements on the Z resonance*, *Phys. Rept.* **427** (2006) 257 [hep-ex/0509008] [INSPIRE].

[48] P. Janot and S. Jadach, *Improved Bhabha cross section at LEP and the number of light neutrino species*, *Phys. Lett. B* **803** (2020) 135319 [arXiv:1912.02067] [INSPIRE].

[49] CDF collaboration, *Measurements of inclusive W and Z cross sections in $p\bar{p}$ collisions at $\sqrt{s} = 1.96$ TeV*, *J. Phys. G* **34** (2007) 2457 [hep-ex/0508029] [INSPIRE].

[50] LHCb collaboration, *Measurement of forward $W \to e\nu$ production in pp collisions at $\sqrt{s} = 8$ TeV*, *JHEP* **10** (2016) 030 [arXiv:1608.01484] [INSPIRE].

[51] ATLAS collaboration, *Precision measurement and interpretation of inclusive W^+, W^- and Z/γ^* production cross sections with the ATLAS detector*, *Eur. Phys. J. C* **77** (2017) 367 [arXiv:1612.03016] [INSPIRE].

[52] D0 collaboration, *A measurement of the $W \to \tau\nu$ production cross section in $p\bar{p}$ collisions at $\sqrt{s} = 1.8$ TeV*, *Phys. Rev. Lett.* **84** (2000) 5710 [hep-ex/9912065] [INSPIRE].

[53] ATLAS collaboration, *Test of the universality of τ and μ lepton couplings in W-boson decays with the ATLAS detector*, *Nature Phys.* **17** (2021) 813 [arXiv:2007.14040] [INSPIRE].

[54] D. d'Enterria and C. Yan, *Revised QCD effects on the $Z \to b\bar{b}$ forward-backward asymmetry*, arXiv:2011.00530 [INSPIRE].

JHEP05(2022)133

[55] CMS collaboration, *Measurement of the t-channel single-top-quark production cross section and of the $|V_{tb}|$ CKM matrix element in pp collisions at $\sqrt{s} = 8$ TeV*, *JHEP* **06** (2014) 090 [arXiv:1403.7366] [INSPIRE].

[56] D0 collaboration, *Measurement of $\sin^2\theta^{\ell}_{\rm eff}$ and Z-light quark couplings using the forward-backward charge asymmetry in $p\bar{p} \to Z/\gamma^* \to e^+e^-$ events with $\mathcal{L} = 5.0\,fb^{-1}$ at $\sqrt{s} = 1.96$ TeV*, *Phys. Rev. D* **84** (2011) 012007 [arXiv:1104.4590] [INSPIRE].

[57] ATLAS collaboration, *Measurement of the effective leptonic weak mixing angle using electron and muon pairs from Z-boson decay in the ATLAS experiment at $\sqrt{s} = 8$ TeV*, Tech. Rep. ATLAS-CONF-2018-037, CERN, Geneva, Switzerland (2018).

[58] SLD collaboration, *First direct measurement of the parity violating coupling of the Z^0 to the s quark*, *Phys. Rev. Lett.* **85** (2000) 5059 [hep-ex/0006019] [INSPIRE].

JHEP05(2022)133